

LETTER

Modeling of broadband power line communication channel based on transmission line theory and radiation lossDonglin He^{1,2}, Yizhen Wei¹, Shuang Cui³, Wei Hua¹, Xueyu Duan¹, and Liang Liu^{1,4a)}

Abstract One challenge with broadband power line communication is the usage of the unshielded transport channels, which still had many interference factors when used to transmit high-speed data, such as noise, attenuation, reflection, radiation and time-varying impedance. In this paper, a two-wire power line is regarded as a long-line antenna. Based on the transmission line theory, reflection theory and radiation loss of long-line antenna, a theoretical model of two-wire power line communication transfer function has been established. The channel transmission characteristics of a power line network can be obtained with its basic elements, the geometric size, the characteristics of the conductor material and the surrounding medium, the structure of power line network, including the power line length, the number of branches and branch terminal load. In the frequency band of 1–200 MHz, the simulated transfer functions of the proposed model are in accordance with the measured results, which proved that the model could accurately predict the power line channel characteristics, and provides theoretical pre-selection guidance of frequency band, power setting and dynamic range for high-speed broadband power line communication.

Keywords: broadband power line communication (BPLC), radiation loss, transmission line theory, transfer function

Classification: Electromagnetic theory

1. Introduction

Broadband Power Line Communication (BPLC) is a special communication technology that uses widely covered power lines to transmit high-speed data and media signals particularly suitable for some old buildings, enterprises, mines, public venues and some other places with difficulties to renew the wiring network [1, 2, 3]. However, the power line is designed to transmit 50/60 Hz power. When it is used as a high-speed transmission channel, some special characteristics, such as noise interference, electromagnetic radiation, time-varying impedance and attenuation [4, 5, 6, 7], are the bottleneck problem that restrict the data transfer rate and distance of BPLC. The transfer function of a power line channel reflects the affection of these channel characteristics of electromagnetic radiation,

time-varying impedance and attenuation. Therefore, it is necessary to work on the channel characteristics of power line networks as the key factors to improve the quality of BPLC include an appropriate selections of a spectrum band-width, a suitable output signal level of a transmitting terminal, and a properly designed input signal dynamite range in a receiving terminal according to its power line transfer function. Modeling and analyzing the transfer function of a power line network channel becomes an important research in the BPLC field.

These last decade, many researches have studied on the accurate channel transmission characteristics of various power line networks [8, 9, 10, 11, 12, 13, 14, 15, 16, 17, 18, 19, 20, 21, 22, 23]. The top-down or bottom-up modeling methods are widely used to build the Power Line Communication (PLC) channel models [9, 10]. A PLC channel model with lattice structure operating in the frequency band of 1–30 MHz is presented in [20], and where the measured impedance and attenuation factors were published in [15]. A simulation of a certain indoor power line network has been achieved without compare with measured results [21]. Another ADS and CST models within an extended the frequency up to 1.3 GHz have been simulated, which different from the measured results [22]. In [23], the power line radiation is described as a dipole antenna. The ABCD method is used to calculate the channel transfer function of the relay assisted PLC channel in [24]. Based on the top-down approach, an analytical PLC channel transfer function formula with a limited set of parameters is established within the frequency band below 500 kHz [25]. Based on the transmission line theory, in [26] presents a frequency dependent causal RLGC (f) model at 1–50 MHz by testing the S-parameters of a three-phase four-wire busbar distribution system.

Despite these achievements on the PLC, the channel model still needs to be further studied in order to accurately estimate the channel attenuation and Spectrum characteristics of a complex power line networks, and provide a guidance of PLC band pre-selection, power setting and dynamic range selection. A radiation PLC transfer function model based on the transmission and radiation theory is proposed in this paper.

This paper is organized as follows: Section 2 will illustrate some foundation concepts to build the power line BPLC model, including the transmission line theory and the long wire antenna radiation theory. Section 3 will analyze the reflection factors along the main line at different branches, calculate the transmission efficiency of a

¹College of Electronics and Information Engineering at Sichuan University, Chengdu 610065, China

²Second Research Institute of Civil Aviation Administration of China, Chengdu 610041, China

³Nanjing Changfeng Aerospace Electronics Technology Company, Nanjing 210000, China

⁴College of Cybersecurity at Sichuan University, Chengdu 610207, China

a) liangzhai118@163.com

DOI: 10.1587/elex.16.20190370

Received June 6, 2019

Accepted June 21, 2019

Publicized July 12, 2019

Copyedited August 25, 2019

PLC channel and present the transfer function model. In Section 4, the accuracy of the proposed irradiate model is elucidated by comparing the simulations with the measured results. Finally, the contribution of the research is given in Section 5.

2. Parameters of parallel two-wire power line

2.1 Equivalent distribution parameters

A two-wire power line is regarded as a parallel two-wire transmission line with evenly distributed parameters in this paper. The distributed parameters per unit length can be stated as Inductance L , Capacitance C , Resistance R , and Conductivity G

$$L = \frac{\mu}{\pi} \ln \frac{D + \sqrt{D^2 - d^2}}{d} \quad (1)$$

$$C = \frac{\pi\epsilon}{\ln \frac{D + \sqrt{D^2 - d^2}}{d}} \quad (2)$$

$$R = \frac{2}{\pi d} \sqrt{\frac{\omega\mu}{2\sigma_2}} \quad (3)$$

$$G = \frac{\pi\sigma_1}{\ln \frac{D + \sqrt{D^2 - d^2}}{d}} \quad (4)$$

Where, μ is the permeability of the medium between the two-wires, D is the distance between the two-wires, d is the diameter of the wire, ϵ is the permittivity of medium between the two-wires, $\omega = 2\pi f$ is the angular frequency, f is the operating frequency, σ_2 is the conductivity of the wire, and σ_1 is the equivalent conductivity of the medium between the two-wires.

The characteristic impedance Z_0 and propagation constant γ [27] of a parallel two-wire power line are defined as

$$Z_0 = \sqrt{\frac{R + j\omega L}{G + j\omega C}} \quad (5)$$

$$\gamma = \sqrt{(R + j\omega L)(G + j\omega C)} = \alpha + j\beta \quad (6)$$

Where, α is the attenuation constant, and β is the phase constant.

2.2 Modification of propagation constant for radiation loss

According to the electromagnetic theory, any signal transmitted in the power line network causes an electromagnetic radiation to the environment, and a power line can be regarded as an antenna [28]. The electromagnetic energy will attenuate during the transmission via the power line due to the radiation. The irradiate attenuation could be equivalent to an ohmic loss on the line. In order to simplify analyze, it is premised that each segment of the power line could be approximately equivalent to a different antenna, although the structure of the power line network are complex. Suppose that the parallel two-wire transmission line could be equivalent as a long wire antenna and its mirror image under the ground [29], as shown in Fig. 1, the

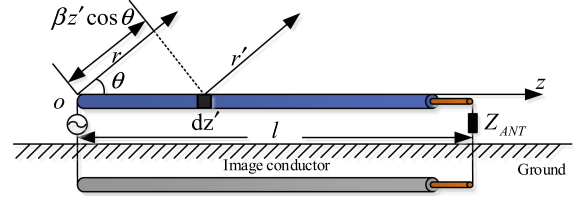


Fig. 1. Long wire antenna.

radiation loss can be imported into the transfer function model of power line channel.

If the transmission current I_0 , on a long wire antenna with a length of l , is constant, which means a constant amplitude with a continuous phase lag. The attenuation of the current on the line is ignored in this paper. The antenna is placed along the z axis, with the feeding point placed at the origin of the coordinate, as shown in Fig. 1. The far-zone radiation field E_θ of the antenna is

$$\begin{aligned} E_\theta &= j\eta \frac{I_0}{2\lambda r} e^{-j\beta r} \sin \theta \int_0^l e^{-j\beta z'} e^{j\beta z' \cos \theta} dz' \\ &= \eta \frac{I_0 l}{2\lambda r} \sin \theta \operatorname{sinc} \left[\frac{\beta l}{2} (1 - \cos \theta) \right] e^{-j\beta r} e^{-j\frac{\beta l}{2}(1 - \cos \theta)} \end{aligned} \quad (7)$$

Where, $\eta = \sqrt{\mu/\epsilon}$ is the wave impedance, r is the distance from the origin to the field point, θ is the angle between the half-line r and the z axis, λ is the wavelength.

According to the ‘‘Poynting vector method’’ [30], if the transmission line has a mismatch impedance load with the traveling wave coefficient K , the antenna radiation power P_r of the traveling wave portion can be obtained

$$\begin{aligned} P_r &= K \iint_s \frac{|E_\theta|^2}{2\eta} \cdot ds \\ &= KI_0^2 \frac{\eta}{4\pi} \left[\ln(2\beta l) - 0.4229 - C_i(2\beta l) + \frac{\sin(2\beta l)}{2\beta l} \right] \end{aligned} \quad (8)$$

Where, $C_i(2\beta l)$ is

$$C_i(2\beta l) = \int_\infty^{2\beta l} \frac{\cos \tau}{\tau} d\tau \quad (9)$$

The radiated power could be considered as an ohmic loss evenly distributed over the antenna. Therefore, the loss resistance R_r per unit length is

$$R_r = K \frac{\eta}{2\pi l} \left[\ln(2\beta l) - 0.4229 - C_i(2\beta l) + \frac{\sin(2\beta l)}{2\beta l} \right] \quad (10)$$

The radiation loss factor could be introduced into the propagation constant γ'

$$\gamma' = \sqrt{(R + R_r + j\omega L)(G + j\omega C)} \quad (11)$$

3. PLC channel model

As an example, a PLC network with N branches ($N \in (0, \infty)$), as shown in Fig. 2, is chosen to analyze the impacts of the load impedance and reflection at the nodes on the transfer function. Notice that each power line segment is regarded as a segment of a transmission line.

The shortest path between the signal source terminal and the load terminal is chosen to be the main line, which is divided into $N + 1$ segments by N nodes. Set the single

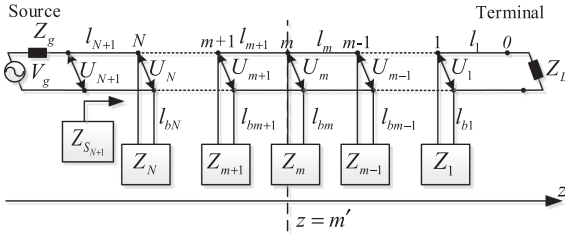


Fig. 2. Multi-Branch PLC network.

source voltage V_g , the internal resistance Z_g . And U_m represents the voltage at the m th node, the m th main line segment length is l_m , the m th branch length is l_{bm} , the main line terminal load is Z_L , and the m th branch load is Z_m . It is assumed that the characteristic impedance of each segment is Z_0 to simplify the analysis in this paper.

Therefore, the ratio of U_m to U_{m+1} can be obtained as

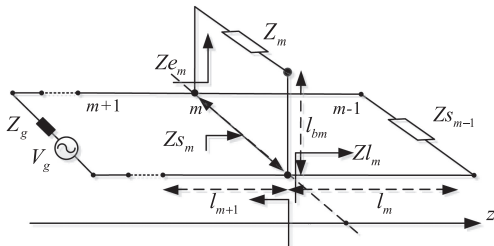
$$\frac{U_m}{U_{m+1}} = \frac{(1 + \Gamma_m)e^{-\gamma' l_{m+1}}}{1 + \Gamma_m e^{-2\gamma' l_{m+1}}} \quad (12)$$

Where, Γ_m is the reflection coefficient at the $z = m'$ plane, and then the equality could obtain the traveling wave coefficient K_m .

$$\Gamma_m = \frac{Z_{S_m} - Z_0}{Z_{S_m} + Z_0} \quad (13)$$

$$K_m = \frac{1 - |\Gamma_m|}{1 + |\Gamma_m|} \quad (14)$$

The reflection analysis starts from Z_L to Z_S along the main line. The input impedance Z_{S_m} at the $z = m'$ plane equal to the parallel connection of Z_{l_m} and Z_{e_m} . Where, Z_{l_m} is the input impedance of the segment l_m with the load $Z_{S_{m-1}}$ ($Z_{S_{m-1}}$ by recursive relations are obtain), and Z_{e_m} is the input impedance of the branch l_{bm} with the load Z_m , as shown in Fig. 3.


 Fig. 3. Input impedance Z_{S_m} parameterization.

$$Z_{S_m} = \frac{Z_{l_m} Z_{e_m}}{Z_{l_m} + Z_{e_m}} \quad (15)$$

$$Z_{l_m} = Z_0 \frac{Z_{S_{m-1}} \cosh(\gamma' l_m) + Z_0 \sinh(\gamma' l_m)}{Z_0 \cosh(\gamma' l_m) + Z_{S_{m-1}} \sinh(\gamma' l_m)} \quad (16)$$

$$Z_{e_m} = Z_0 \frac{Z_m \cosh(\gamma' l_{bm}) + Z_0 \sinh(\gamma' l_{bm})}{Z_0 \cosh(\gamma' l_{bm}) + Z_m \sinh(\gamma' l_{bm})} \quad (17)$$

Notice that, at the signal source plane, there are

$$\frac{U_{N+1}}{V_g} = \frac{Z_{S_{N+1}}}{Z_{S_{N+1}} + Z_g} \quad (18)$$

Therefore, the ratio of the source voltage to the terminal voltage is obtained

$$\frac{U_0}{V_g} = \frac{U_{N+1}}{V_g} \frac{U_N}{U_{N+1}} \dots \frac{U_m}{U_{m+1}} \dots \frac{U_1}{U_2} \frac{U_0}{U_1} \quad (19)$$

The transfer function $H(f)$ of power line networks with wave source and terminal load is

$$H(f) = 2 \frac{U_0}{V_g} \quad (20)$$

4. Comparison of simulated and measured results

Different PLC test cases are selected to compare the simulated and measured results. Each case has different power line lengths, number of branches and branch terminal load impedances of $\{5.3 \Omega, 50.8 \Omega, 1197 \Omega, \infty\}$ to represent impedances of low, RF standard, high, and open circuit (∞ , OC), respectively [31].

The parameters of the two-wire power line ($2 \times 1 \text{ mm}^2$) are listed in Table I. The parameters of the single-branch, double-branch and multi-branch networks cases are shown in Fig. 2, as shown in Table II, III and IV.

Table I. Parameters of the selected two-wire power line.

Parameter	D	d	σ_1	σ_2	μ	ϵ
Value	2.6	1.13	10^{-8}	5.88×10^7	$4\pi \times 10^{-7}$	$(1.25/36\pi) \times 10^{-9}$
Unit	mm	mm	S/m	S/m	H/m	F/m

A Vector Network Analyzer is utilized to measure the test cases, as shown in Fig. 4. The Tx port of the power line network is connected to port A (port impedance is 50Ω) and the Rx port is connected to port B (port impedance is 50Ω).

The scattering parameters S_{21} of different cases are tested. The calculated modeling results and the experimental results are shown in Fig. 6, 8 and 10 to verify the validity of the model.

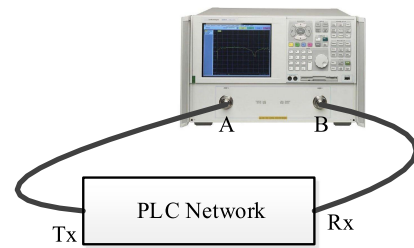


Fig. 4. Schematic diagram of measurement setup.

4.1 Single-branch network

Fig. 5 is a diagrammatic sketch of a single-branch network, whose parameters are shown in Table II, $Z_g = Z_l = 50 \Omega$.

Fig. 6-(a), (b), (c), (d) show the comparison of the basic model simulated results (no radiation loss), the radiation model simulated results and measured results on the single branch network in the frequency range of 1–200 MHz with the load impedances $Z_1 = \text{OC}, 1197 \Omega, 50.8 \Omega, 5.3 \Omega$, respectively.

The measured results with different Z_1 are highly consistent with that of the radiation model. It proves that

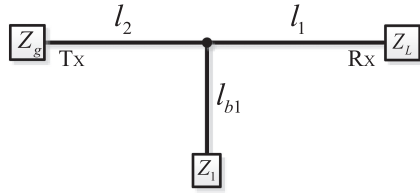
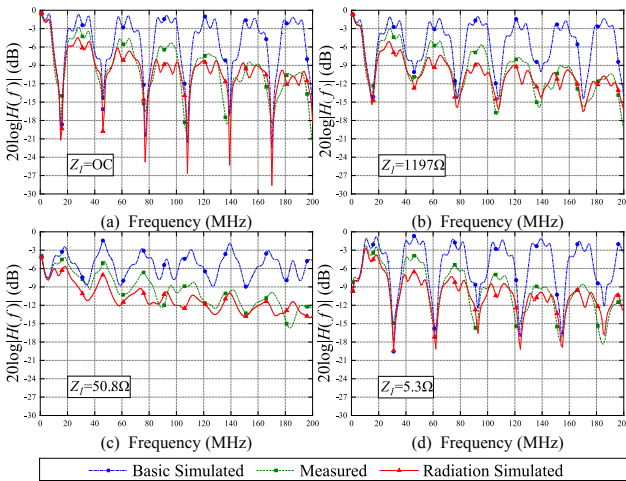


Fig. 5. Single-branch network.

Table II. Single-branch network parameters.

No.	l_2 (m)	l_1 (m)	l_{b1} (m)	Z_1 (Ω)
(1)	4	6	3	OC, 1197, 50.8, 5.3


 Fig. 6. Single-branch network with different Z_1 -(1).

the different load impedances have different groove depths and indicates that the radiation model are correct and effective.

4.2 Double-branch network

The diagrammatic sketch of double-branch network is shown in Fig. 7, and the parameters of the network are listed in Table III, $Z_g = Z_l = 50 \Omega$.

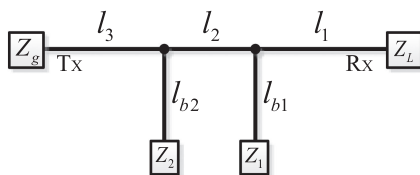


Fig. 7. Double-branch network.

Table III. Double-branch network parameters.

No.	l_3 (m)	l_2 (m)	l_1 (m)	l_{b2} (m)	l_{b1} (m)	Z_2 (Ω)	Z_1 (Ω)
(2)	4	3	3	3	1	OC	OC
						1197	5.3
						50.8	OC

The measured results and radiation simulated results of the double-branch network are shown in Fig. 8. For the double-branch network, radiation simulated results was compared with experimental ones, which also proves the validity of model verified.

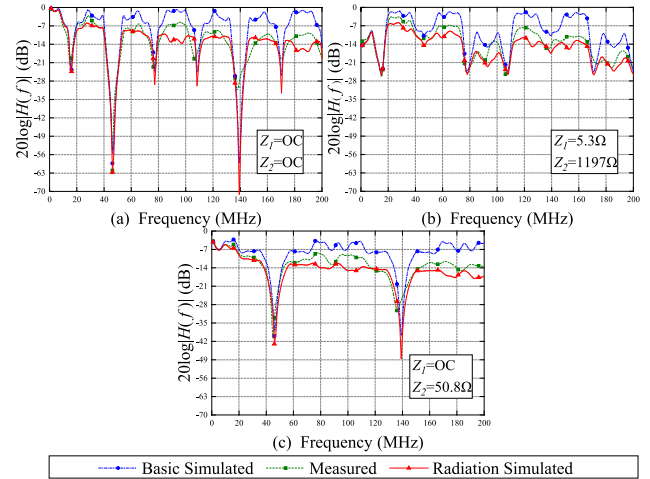
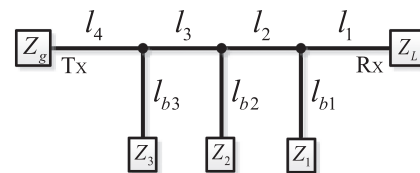

 Fig. 8. Double-branch network with different Z_1 and Z_2 -(2).


Fig. 9. Three-branch network.

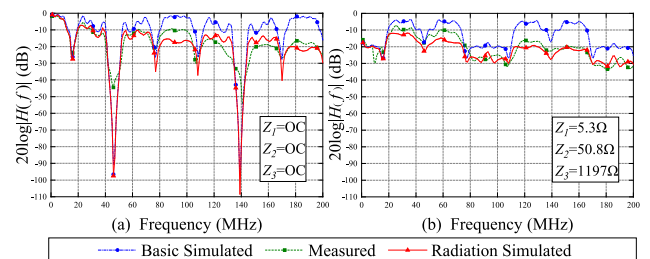
Table IV. Three-branch network parameters.

No.	l_4 (m)	l_3 (m)	l_2 (m)	l_1 (m)	l_{b3} (m)	l_{b2} (m)	l_{b1} (m)	Z_3 (Ω)	Z_2 (Ω)	Z_1 (Ω)
(3)	4	3	5	3	3	1	1	OC	OC	OC
								1197	50.8	5.3

4.3 Three-branch network

One three-branch network example is shown in Fig. 9 with the parameters listed in Table IV, $Z_g = Z_l = 50 \Omega$.

Fig. 10 shows the measured results and radiation model simulated results of the three-branch network. Similarly, the positions of attenuation notches of the measured results coincided well with the radiation simulated results in multiple branches networks. This consistency of the attenuation notches shows that this radiation model could correctly reflect a channel transfer characteristics of power line networks.


 Fig. 10. Measured and simulated results of Three-branch network with different Z_1 , Z_2 and Z_3 -(3).

5. Conclusion

A novel channel transfer function model of power line communication, which is based on the parallel two-line

transmission line theory, is proposed. The transfer function is obtained by calculating the voltage ratio between a source and a terminal in a power line network with a radiation loss of a long wire antenna and a reflection factor in a transmission line with a mismatch load. In the frequency band of 1–200 MHz, the feasibility of the method and the correctness of the proposed model are verified by testing the single-branch, double-branch and three-branch networks with different load impedances. By known the geometry size, the conductor and the surrounding medium characteristics of the power line, the proposed radiate model could obtain the transfer function without attenuation measurement. This radiation model provides a reliable method to predict the attenuation and spectrum grooves of a PLC channel, and also provides a solution for the high-efficiency spectrum usage and the channel attenuation analysis of high-speed BPLC.

Acknowledgments

This work was supported by National Key Research and Development Program of China (Grant No. 2017YFB0308600) and Civil Aviation Joint Fund of the National Natural Science Foundation of China (Grant No. U1733109).

References

- [1] G. Artale, *et al.*: “A new low cost power line communication solution for smart grid monitoring and management,” *IEEE Trans. Instrum. Meas.* **21** (2018) 29 (DOI: [10.1109/MIM.2018.8327976](https://doi.org/10.1109/MIM.2018.8327976)).
- [2] D. P. F. Möller and H. Vakilzadian: “Ubiquitous networks: Power line communication and internet of things in smart home environments,” 2014 IEEE International Conference on Electro/Information Technology (2014) 596 (DOI: [10.1109/EIT.2014.6871832](https://doi.org/10.1109/EIT.2014.6871832)).
- [3] J. Granado, *et al.*: “Modeling airfield ground lighting systems for narrowband powerline communications,” *IEEE Trans. Power Del.* **25** (2010) 2399 (DOI: [10.1109/TPWRD.2010.2054839](https://doi.org/10.1109/TPWRD.2010.2054839)).
- [4] A. G. Lazaropoulos and P. G. Cottis: “Transmission characteristics of overhead medium-voltage power-line communication channels,” *IEEE Trans. Power Del.* **24** (2009) 1164 (DOI: [10.1109/TPWRD.2008.2008467](https://doi.org/10.1109/TPWRD.2008.2008467)).
- [5] Z. Tan, *et al.*: “Noise modelling for power line communication in harsh environment,” *ICISCE* (2017) 1559 (DOI: [10.1109/ICISCE.2017.325](https://doi.org/10.1109/ICISCE.2017.325)).
- [6] H. C. Ferreira, *et al.*: *Power Line Communications: Theory and Applications for Narrowband and Broadband Communications Over Power Lines* (John Wiley & Sons, 2010).
- [7] M. Zimmermann and K. Dostert: “Analysis and modeling of impulsive noise in broadband power line communications,” *IEEE Trans. Electromagn. Compat.* **44** (2002) 249 (DOI: [10.1109/15.990732](https://doi.org/10.1109/15.990732)).
- [8] J. Shin, *et al.*: “Channel modeling for indoor broadband power-line communications networks with arbitrary topologies by taking adjacent nodes into account,” *IEEE Trans. Power Del.* **26** (2011) 1432 (DOI: [10.1109/TPWRD.2010.2103331](https://doi.org/10.1109/TPWRD.2010.2103331)).
- [9] M. Zimmermann and K. Dostert: “A multipath model for the powerline channel,” *IEEE Trans. Commun.* **50** (2002) 553 (DOI: [10.1109/26.996069](https://doi.org/10.1109/26.996069)).
- [10] H. Meng, *et al.*: “A transmission line model for high-frequency power line communication channel,” *POWERCON* (2002) 1290 (DOI: [10.1109/ICPST.2002.1047610](https://doi.org/10.1109/ICPST.2002.1047610)).
- [11] A. M. Tonello, *et al.*: “A top-down random generator for the in-home PLC channel,” *GLOBECOM* (2011) 1 (DOI: [10.1109/GLOCOM.2011.6133815](https://doi.org/10.1109/GLOCOM.2011.6133815)).
- [12] S. Galli: “A novel approach to the statistical modeling of wireline channels,” *IEEE Trans. Commun.* **59** (2011) 1332 (DOI: [10.1109/TCOMM.2011.031611.090692](https://doi.org/10.1109/TCOMM.2011.031611.090692)).
- [13] A. M. Tonello, *et al.*: “A fitting algorithm for random modeling the PLC channel,” *IEEE Trans. Power Del.* **27** (2012) 1477 (DOI: [10.1109/TPWRD.2012.2196714](https://doi.org/10.1109/TPWRD.2012.2196714)).
- [14] K. Khalil, *et al.*: “An MIMO random channel generator for indoor power-line communication,” *IEEE Trans. Power Del.* **29** (2014) 1561 (DOI: [10.1109/TPWRD.2014.2331078](https://doi.org/10.1109/TPWRD.2014.2331078)).
- [15] M. Mosalaosi and T. J. O. Afullo: “A deterministic channel model for multi-access broadband powerline communication,” *Africon* (2015) 1 (DOI: [10.1109/AFRCON.2015.7331993](https://doi.org/10.1109/AFRCON.2015.7331993)).
- [16] A. M. Tonello and T. Zheng: “Bottom-up transfer function generator for broadband PLC statistical channel modeling,” *SPLC* (2009) 7 (DOI: [10.1109/ISPLC.2009.4913395](https://doi.org/10.1109/ISPLC.2009.4913395)).
- [17] F. Versolatto and A. M. Tonello: “An MTL theory approach for the simulation of MIMO power line communication channels,” *IEEE Trans. Power Del.* **26** (2011) 1710 (DOI: [10.1109/TPWRD.2011.2126608](https://doi.org/10.1109/TPWRD.2011.2126608)).
- [18] A. M. Tonello and F. Versolatto: “Bottom-up statistical PLC channel modeling—Part II: Inferring the statistics,” *IEEE Trans. Power Del.* **25** (2010) 2356 (DOI: [10.1109/TPWRD.2010.2053561](https://doi.org/10.1109/TPWRD.2010.2053561)).
- [19] S. Souissi, *et al.*: “Bottom-up approach for narrowband powerline channel modeling,” *GLOBECOM* (2013) 2987 (DOI: [10.1109/GLOCOM.2013.6831529](https://doi.org/10.1109/GLOCOM.2013.6831529)).
- [20] M. Mosalaosi and T. J. O. Afullo: “Channel modeling for high-speed indoor powerline communication systems: The lattice approach,” *Ann. Telecommun.* **72** (2017) 499 (DOI: [10.1007/s12243-016-0554-3](https://doi.org/10.1007/s12243-016-0554-3)).
- [21] P. J. Joseph and S. S. Pillai: “Modeling of broadband power line communication in last-mile networks,” *COMSNETS* (2016) 137 (DOI: [10.1109/CSN.2016.7824002](https://doi.org/10.1109/CSN.2016.7824002)).
- [22] A. H. Y. Rashid, *et al.*: “A simple propagation model for broadband powerline communications system,” *ICIAS* (2012) 307 (DOI: [10.1109/ICIAS.2012.6306207](https://doi.org/10.1109/ICIAS.2012.6306207)).
- [23] C. J. Kikkert, *et al.*: “Radiation and attenuation of communication signals on power lines,” *ICICS* (2009) (DOI: [10.1109/ICICS.2009.5397568](https://doi.org/10.1109/ICICS.2009.5397568)).
- [24] X. Wu, *et al.*: “Channel model proposal for indoor relay-assisted power line communications,” *IET Commun.* **12** (2018) 1236 (DOI: [10.1049/iet-com.2017.0782](https://doi.org/10.1049/iet-com.2017.0782)).
- [25] H. Gassara, *et al.*: “Top-down random channel generator for the narrowband power line communication,” *AEU Int. J. Electron. Commun.* **89** (2018) 146 (DOI: [10.1016/j.aeue.2018.03.003](https://doi.org/10.1016/j.aeue.2018.03.003)).
- [26] Z. Hasirci and I. H. Cavdar: “S-parameters-based causal RLGC (f) model of busbar distribution systems for broadband power line communication,” *Int. J. Electr. Power Energy Syst.* **95** (2018) 561 (DOI: [10.1016/j.ijepes.2017.09.015](https://doi.org/10.1016/j.ijepes.2017.09.015)).
- [27] K. Cheng: *Field and Wave Electromagnetics* (Addison-Wesley, 1989).
- [28] F. Sekyere: “Signal radiation leakage of power line communication systems,” M.S. dissertation, Kwame Nkrumah University of Science and Technology, Ghana (1993).
- [29] H. Ward Silver: *The ARRL Antenna Book for Radio Communications* (The National Association for Amateur Radio, Newington, USA, 2011) 22nd ed.
- [30] J. D. Kraus and R. J. Marhefka: *Antennas: For All Applications* (McGraw-Hill, New York, 2002) 3rd ed.
- [31] F. J. Canete, *et al.*: “A channel model proposal for indoor power line communications,” *IEEE Commun. Mag.* **49** (2011) 166 (DOI: [10.1109/MCOM.2011.6094022](https://doi.org/10.1109/MCOM.2011.6094022)).